



OPEN

A comprehensive analysis of the role of QPRT in breast cancer

Yiqing Yan^{1,3}, Lun Li^{1,3}, Zixin Wang¹, Jian Pang¹, Xinyu Guan¹, Yunchang Yuan², Zhenkun Xia²✉ & Wenjun Yi¹✉

To explore the clinical role of QPRT in breast cancer. The gene expression, methylation levels and prognostic value of QPRT in breast cancer was analyzed using TCGA data. Validation was performed using the data from GEO dataset and TNMPLOT database. Meta analysis method was used to pool the survival data for QPRT. The predictive values of QPRT for different drugs were retrieved from the ROC plot. The expression differences of QPRT in acquired drug-resistant and sensitive cell lines were analyzed using GEO datasets. GO and KEGG enrichment analysis were conducted for those genes which were highly co-expressed with QPRT in tissue based on TCGA data and which changed after QPRT knockdown. Timer2.0 was utilized to explore the correlation between QPRT and immune cells infiltration, and the Human Protein Atlas was used to analyse QPRT's single-cell sequencing data across different human tissues. The expression of QPRT in different types of macrophages, and the expression of QPRT were analysed after coculturing HER2+ breast cancer cells with macrophages. Additionally, TargetScan, Comparative Toxicogenomics and the connectivity map were used to research miRNAs and drugs that could regulate QPRT expression. Cytoscape was used to map the interaction networks between QPRT and other proteins. QPRT was highly expressed in breast cancer tissue and highly expressed in HER2+ breast cancer patients ($P < 0.01$). High QPRT expression levels were associated with worse OS, DMFS, and RFS ($P < 0.01$). Two sites (cg02640602 and cg06453916) were found to be potential regulators of breast cancer ($P < 0.01$). QPRT might predict survival benefits in breast cancer patients who received taxane or anthracycline. QPRT was associated with tumour immunity, especially in macrophages. QPRT may influence the occurrence and progression of breast cancer through the PI3K-AKT signalling pathway, Wnt signalling pathway, and cell cycle-related molecules.

Data from the International Agency for Research on Cancer (IARC) show that breast cancer has become the highest incidence of malignant tumours in the world and one of the leading causes of death in women¹. Breast cancer is classified into different biological subtypes with complex heterogeneity. In clinical practice, there are four common molecular types, including luminal-A, luminal-B, human epidermal growth factor receptor 2 (HER2)-positive and triple-negative², leading to various treatments³. Although breast cancer is one of the solid tumours with the best treatment effects, the heterogeneity of different breast cancer molecular subtypes leads to different treatments⁴, making it difficult to accomplish personalized precision therapy in patients.

Despite great progress in present frontal and effective treatments, systemic therapy still cannot completely cure metastatic breast cancer to improve quality of life⁵, alleviate symptoms caused by metastasis, and prolong relative long-term survival⁶. Considering the significant mortality rate, it is essential to explore new therapies for inhibiting the development of malignant systemic metastasis. The biggest challenge in the treatment of metastatic breast cancer is resistance to systemic chemotherapy and targeted therapy, which has been insurmountable thus far. Metastatic breast cancer must be treated on an individualized basis. Clinically, combined chemotherapy can improve the drug response rate and prolong progression-free survival in some patients. However, the gradual formation of drug resistance causes drug therapy to lose considerable clinical benefits. There are many known mechanisms of drug resistance, including accelerating drug efflux, drug activation and inactivation, drug target changes, and epigenetic modifications produced or obtained by mutations⁷. Several strategies have been designed to prevent or overcome resistance to systemic anticancer therapy, including drug combinations and sequential regimens. However, it seems that resistance to existing drugs and treatment regimens is inevitable in patients⁸. Therefore, we hope to further clarify the cellular and molecular processes of drug resistance in tumour cells,

¹Department of General Surgery, The Second Xiangya Hospital, Central South University, No. 139, Renmin Central Road, Changsha 410011, China. ²Department of Thoracic Surgery, The Second Xiangya Hospital, Central South University, No. 139, Renmin Central Road, Changsha 410011, China. ³These authors contributed equally: Yiqing Yan and Lun Li. ✉email: xwvfye@126.com; yiwenjun@csu.edu.cn

use new drugs to combat these mechanisms, and gradually improve the prognosis of patients with metastatic breast cancer⁹.

Quinolate phosphoribosyltransferase (QPRT) is a key enzyme for tryptophan degradation to nicotinamide adenine dinucleotide (NAD⁺), collectively known as the kynurenine pathway. NAD⁺ is a coenzyme of many dehydrogenases in the human body, which can transfer electrons and connect the tricarboxylic acid cycle and respiratory chain. The function of NAD⁺ is to transfer the removed hydrogenic ionization to flavoprotein during the metabolic process. Ullmark et al. found that overexpression of QPRT in K562 cells increased drug resistance to imatinib and suggested that QPRT is a new direct target gene of WT1 in leukaemia cells¹⁰. Moreover, the overexpression of QPRT promoted the growth, migration, and invasion of estrogen receptor (ER)-positive BC cells¹¹.

Therefore, in this study, QPRT was studied in terms of its expression, regulation, and interaction as well as its effect on prognosis in BC tissue by TCGA data, which provided an experimental basis for further exploring the molecular mechanisms of QPRT and a reference for clinical diagnosis, treatment and prognosis in BC.

Materials and methods

The expression data of QPRT and gene correlation analysis. Expression data of the QPRT gene were obtained from several databases, including the UALCAN database¹², bc-GenExMiner database¹³, TNM-PLOT database¹⁴, and multiple breast cancer-related GEO datasets. Differential expression analysis of QPRT in different clinical and pathological factors, such as tumour stage, breast cancer subgroups, lymph node metastasis, and TP53 mutations, was performed using the UALCAN online database and bc-GenExMiner database. The relationships between QPRT expression levels and overall survival (OS), distant metastasis-free survival (DMFS), and relapse-free survival (RFS) were explored by Kaplan–Meier plotter¹⁵ and bc-GenExMiner. The data from multiple datasets were combined using a meta-analysis approach to analyse the relationship between QPRT expression levels and survival.

Using the linkedomics database¹⁶, GSE151521 dataset¹⁷, and Cytoscape, QPRT-related genes were selected. Subsequently, the DAVID online analysis tool¹⁸ and KOBAS¹⁹ were utilized to perform GO and KEGG enrichment analysis²⁰ on these genes, aiming to elucidate the potential signalling pathways and biological processes that may be affected.

Analysis of QPRT methylation levels. Based on TCGA (The Cancer Genome Atlas) data on the MethSurv²¹ online database and Wanderer²², the relationship among methylation sites, QPRT expression, and survival analysis was performed between breast cancer tissue and normal tissue.

Predictive values of QPRT in cancer treatments. According to ROCplot²³, the predictive values of QPRT in different breast cancer treatments were obtained. The final outcomes with RFS at 5 years and pathological complete response (pCR) in different therapies were able to predict the breast cancer patients' survival values.

QPRT expression in tumour-acquired drug resistance. By downloading data from multiple GEO datasets of acquired drug resistance in tumours, including GSE143944, GSE130437, GSE98987, GSE130437, GSE67916, GSE76540, GSE15043, GSE90564, GSE99225, the expression differences of QPRT between drug-sensitive and drug-resistant groups were analyzed.

QPRT single-cell analyses and immune infiltrate abundances in breast cancer. The Human Protein Atlas (HPA)²⁴ was used to explore QPRT expression in different human tissues by single-cell expression correlation analysis. TIMER2.0²⁵ was used to explore the association between immune infiltrates and QPRT expression in TCGA.

Cell culture and real-time quantitative PCR (qPCR). BT-474, SK-BR-3, and THP-1 cells were obtained from Procell with the passing identification of short tandem repeats and qPCR detection of Mycoplasma. The culture media for the BT-474 cell line contained Roswell Park Memorial Institute (RPMI)-1640, 10 µg/ml insulin, 20% foetal calf serum (FBS), and 1% penicillin–streptomycin (P/S). The culture media conditions for the SK-BR-3 cell line contained McCoy's 5A, 10% FBS, and 1% P/S. The culture media for the THP-1 cell line contained RPMI-1640, 10% FBS, 0.05 mM β-mercaptoethanol, and 1% P/S. THP-1 monocytes were induced to differentiate into macrophages by adding PMA (100 ng/ml) to the culture medium for 48 h. Then, macrophages were stimulated with LPS (100 ng/ml) and IFN-γ (20 ng/ml) for 48 h to induce M1 macrophage polarization. The addition of IL-4 (20 ng/ml) and IL-13 (20 ng/ml) for 48 h induced macrophage polarization to M2 macrophages.

Total RNA was extracted by TRIzol reagent (Invitrogen, 15596026) and reverse transcribed by HiScript II Reverse Transcriptase (Vazyme, R212-01). Then, 2X Universal SYBR Green Fast qPCR Mix (ABclonal, RK21203) was used for qPCR detection.

Gene primer sequences used in this study were as follows: QPRT Forwards: 5'-GCTGGTGCCGACCTTGTCCT-3'; Reverse: 5'-TCCACAGCCACACTCGGGAAC-3'; GAPDH Forwards: 5'-AACGGGAAGCTTGTCATCAA-3'; Reverse: 5'-TGGACTCCACGACTACTCA-3'.

Expression targeted regulation of QPRT. The miRNAs that regulate QPRT expression were predicted using the TargetScan online database²⁶. Based on Cytoscape, the genes or protein molecules interacting with QPRT were selected, and a protein–protein interaction (PPI) network was constructed. The Comparative Toxicogenomics Database²⁷ and the connectivity map²⁸ were used to identify targeted drugs that affect pathogenesis and tumour progression in breast cancer.

Statistical analysis. Experimental data are presented as the mean \pm 95% CI, and were analysed using GraphPad Prism 9.0 software. Two-tailed unpaired Student's *t*-test was used to calculate *P* values. A two-tailed *P* value of 0.05 was considered statistically significant. The expression data of QPRT were retrieved from GEO datasets, and its prognostic values in terms of overall survival, recurrence-free survival, DMFS, and disease-free survival were analysed using SPSS software. Data from several datasets for the same outcomes were pooled using Revman Software. The fixed effect model was used if the heterogeneity was small ($I^2 < 40\%$); otherwise, the random effect model was used.

Patient and public involvement statement. Patients or the public were not involved in the design, conduct, reporting, or dissemination plans of our research.

Results

The expression and characteristics of QPRT in breast cancer tissue. Based on The Cancer Genome Atlas (TCGA) datasets, the expression of QPRT was significantly higher in BC tissue than in normal breast tissue ($P < 0.0001$) (Fig. 1A–B). In terms of clinical characteristics, high expression of QPRT was correlated with lymph node metastasis (all $P < 0.05$) (Fig. 1C), and high QPRT expression levels were associated with nodal positive statuses (Fig. S1A) and mutated P53 (Fig. S1B) in the Gene Expression Omnibus (GEO) databases.

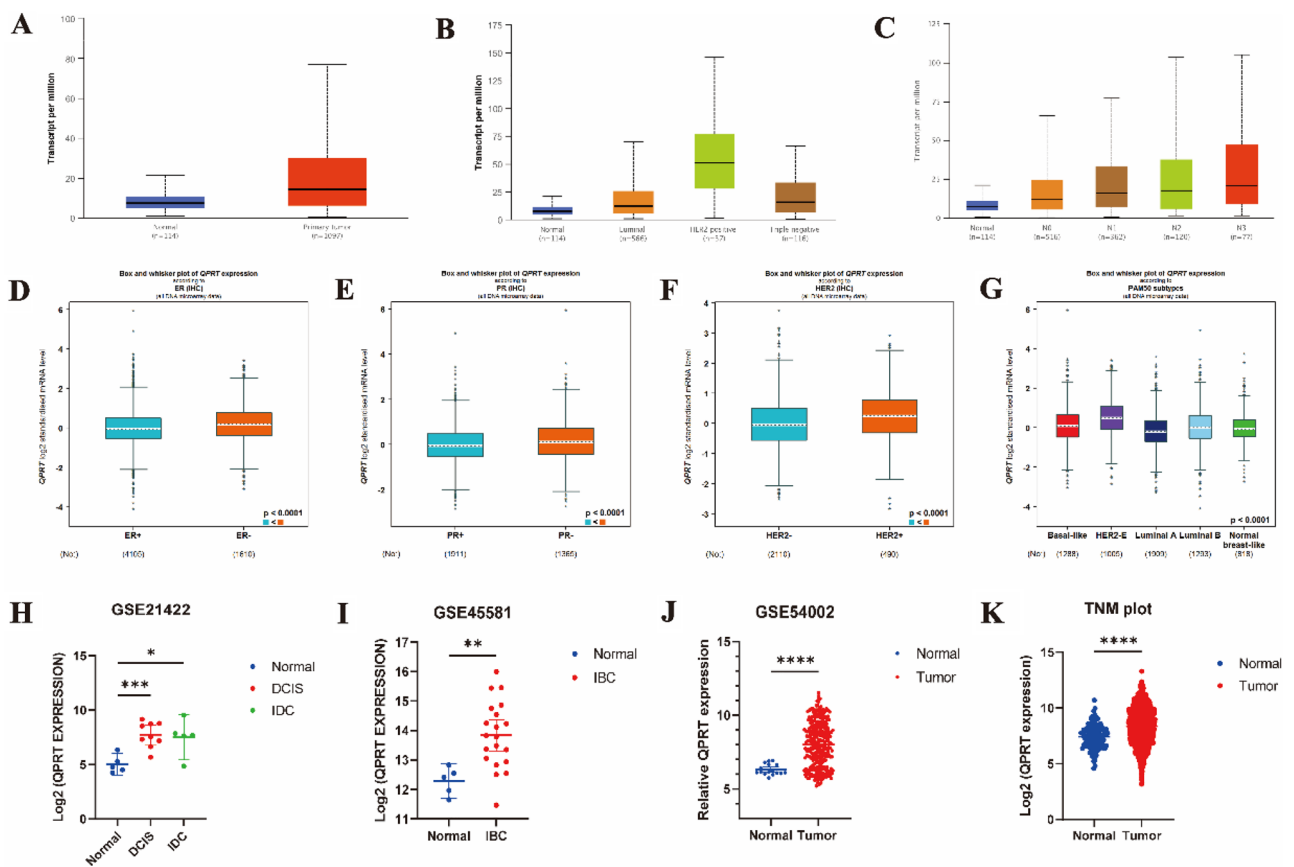


Figure 1. The expression and characteristics of QPRT in breast cancer tissue. (A) The QPRT expression differences between normal and primary tumor tissues in BRCA were compared using UALCAN. (B) The expression of QPRT across different subclasses of breast cancer in TCGA was analyzed by the UALCAN database. (C) The expression of QPRT in breast cancer about different node statuses in TCGA was analyzed by the UALCAN database. (D) The expression of QPRT between ER+ and ER- breast cancer in GEO using the bc-GenExMiner database. (E) The expression of QPRT between PR+ and PR- breast cancer in GEO using the bc-GenExMiner database. (F) The expression of QPRT between HER2+ and HER2- breast cancer in GEO using the bc-GenExMiner database. (G) The expression of QPRT across different PAM50 subtypes of breast cancer in GEO using the bc-GenExMiner database. (H) Log₂ gene expression of QPRT gene in DCIS and IDS patients compared to healthy samples in GSE21422. (I) Log₂ gene expression of QPRT gene in IBC patients compared to healthy samples in GSE45581. (J) Gene expression of QPRT gene in patients with breast cancer compared to healthy samples in GSE54002. (K) Log₂ gene expression of QPRT gene in BRCA patients compared to healthy samples in TNM plot. Two-tailed unpaired Student's *t*-test was used to calculate *P* values. (H)–(K) Data are presented as the mean \pm 95% CI. * $P < 0.05$; ** $P < 0.01$; *** $P < 0.001$, **** $P < 0.0001$. BRCA: Breast invasive carcinoma, CI: Confidence interval, DCIS: The ductal carcinoma in situ, IBC: Inflammatory breast cancer, IDS: Invasive ductal carcinoma.

As shown in GEO databases, ER-negative (ER⁻), progesterone receptor-negative (PR⁻), and HER2-positive (HER2⁺) breast cancer patients had high QPRT expression ($P < 0.0001$) (Fig. 1D–F). In the molecular subtyping of breast cancer, HER2⁺ breast cancer patients had higher QPRT expression than luminal A/B and TNBC patients ($P < 0.01$) (Fig. 1B). Furthermore, HER2⁺ breast cancer patients had the highest level of QPRT, which was much higher than that in luminal B breast cancer patients ($P < 0.0001$). Basal-like breast and normal breast-like cancer patients were lower than HER2⁺ breast cancer patients. Luminal A breast cancer patients had the lowest QPRT expression (Fig. 1G). To verify QPRT expression in BC tissue and normal breast tissue, we included different GEO gene expression datasets and TNMplot datasets in our analysis. We found that QPRT was more highly expressed in BC tissue than in normal breast tissue within these datasets (Fig. 1H–K).

The relationship between QPRT expression and prognosis in breast cancer. The results from the Kaplan–Meier plotter revealed that breast cancer patients with high QPRT levels had shorter overall survival (OS) (HR 1.38, 95% CI 1.14–1.67, $P = 0.01$) (Fig. 2A), distant metastasis-free survival (DMFS) (HR 1.59, 95% CI 1.36–1.86, $P < 0.01$) (Fig. 2B) and relapse-free survival (RFS) (HR 1.40, 95% CI 1.26–1.56, $P < 0.01$) (Fig. 2C). The analysis results from the bc-GenExMiner database also confirmed that patients with the high QPRT expression had worse OS, DMFS, and RFS than those with the low QPRT expression ($P < 0.0001$). The prognostic results were consistent among ER⁺, PR⁺, and HER2⁺ receptor statuses and different intrinsic molecular subtypes ($P < 0.05$) (Fig. S2).

In addition, we used meta-analysis methods to pool data from multiple datasets to analyse the relationship between QPRT expression level and survival. Ten datasets (2822 samples) assessed the relationship between QPRT and overall survival. The pooled analysis showed that high QPRT might be associated with shorter overall survival (HR 1.35, 95% CI 1.24–1.47, $P < 0.00001$) (Fig. 2D). Eleven datasets (2085 samples) assessed the relationship between QPRT and recurrence-free survival. The pooled analysis showed that high QPRT might be associated with shorter recurrence-free survival (HR 1.19, 95% CI 1.04–1.35, $P = 0.009$) (Fig. 2E). Twelve datasets (3180 samples) assessed the relationship between QPRT and disease-free survival. The pooled analysis showed that high QPRT might be associated with shorter disease-free survival (HR 1.22, 95% CI 1.07–1.39, $P = 0.003$) (Fig. 2F). Seventeen datasets (4100 samples) assessed the relationship between QPRT and distant metastasis-free survival. The pooled analysis showed that high QPRT might be associated with shorter distant metastasis-free survival (HR 1.25, 95% CI 1.17–1.33, $P < 0.00001$) (Fig. 2G).

The methylation level of QPRT and prognosis in breast cancer. Based on TCGA data, the QPRT promoter methylation level was higher in breast cancer tissue than in normal breast tissue ($P < 0.01$) (Fig. 3B). To explore the correlation between the QPRT methylation level and expression in breast cancer, 26 methylation sites were obtained with CpG islands highlighted in green. At three sites, cg16754364, cg00097384, and cg00145955, hypermethylation, compared to the methylation level in normal breast tissue, was observed in tumour tissue and at the other 15 sites, the methylation sites tended to be highly methylated in normal breast tissue rather than in tumour tissue, which meant that they had a poor resolution in detecting hypermethylation in tumours (Fig. 3A). Using MethSurv data, survival analyses showed that two hypermethylation sites of QPRT (cg02640602 and cg06453916) correlated with better prognoses in OS ($P < 0.01$) (Fig. 3C–D).

The predictive values of QPRT in breast cancer treatments. To validate predictive biomarkers in breast cancer, we assessed the relationship between QPRT expression and treatment response. Among those patients who received taxane (AUC = 0.58, $P = 1.2e-02$) or anthracycline (AUC = 0.58, $P = 4.6e-03$), QPRT expression was associated with worse relapse-free survival at 5 years. Among the patients who were administered taxane (AUC = 0.54, $P = 1.1e-02$) or anthracycline (AUC = 0.53, $P = 3.2e-02$), the utilization of QPRT may be indicative of higher rates of pathological complete response (pCR) (Fig. S3). It is worth noting that a higher pCR rate is associated with a poorer prognosis. For patients receiving other therapies (including tamoxifen, an aromatase inhibitor, trastuzumab, lapatinib, ixabepilone, etc.), QPRT might not predict the survival benefits ($P > 0.5$).

The expression of QPRT and acquired drug resistance. In terms of CDK4/6 inhibitors, QPRT might be a resistant biomarker for ribociclib (CAMA-1, GSE143944, $P = 0.0001$) (Fig. 4A) and palbociclib (MDA-MB-231, GSE130437, $P < 0.0001$ & MCF 7, GSE98987, $P < 0.0001$ & MCF-7, GSE130437, $P < 0.0001$) (Fig. 4B–D). QPRT might be a resistant biomarker for tamoxifen (MCF 7, GSE67916, $P = 2.5e-02$) (Fig. 4E), doxorubicin (MCF 7, GSE76540, $P = 1.9e-03$) (Fig. 4F), trastuzumab (BT474, GSE15043, $P = 6.3e-03$) (Fig. 4G), and paclitaxel (MDA-MB-231, GSE90564, $P = 3.4e-02$) resistance (Fig. 4H).

The related genes and function prediction results of QPRT. We obtained 685 genes significantly correlated with QPRT from LinkedOmics database. Among those genes, 368 genes were positively correlated ($r > 0.25$, $P < 0.05$), and 317 genes were negatively correlated ($r < -0.25$, $P < 0.05$).

To elucidate the biological functions and pathways associated with QPRT, GO enrichment and KEGG pathway analyses were performed, and the results showed that related biological processes included regulation of the G1/S transition of the mitotic cell cycle, protein ubiquitination, regulation of the G0–G1 transition, positive regulation of the Wnt signalling pathway and positive regulation of B-cell proliferation (Fig. S4A). For molecular function, QPRT was associated with protein binding, siRNA binding, and glutathione hydrolase activity (Fig. S4B). For cellular components, QPRT was associated with the nucleus, cytoplasm, cytosol, nucleoplasm, and extracellular exosome (Fig. S4C). Furthermore, KEGG pathway analysis indicated that RNA Polymerase II Transcription, generic transcription pathway, TCR signalling, and the ER–phagosome pathway were also enriched (Fig. S4D).

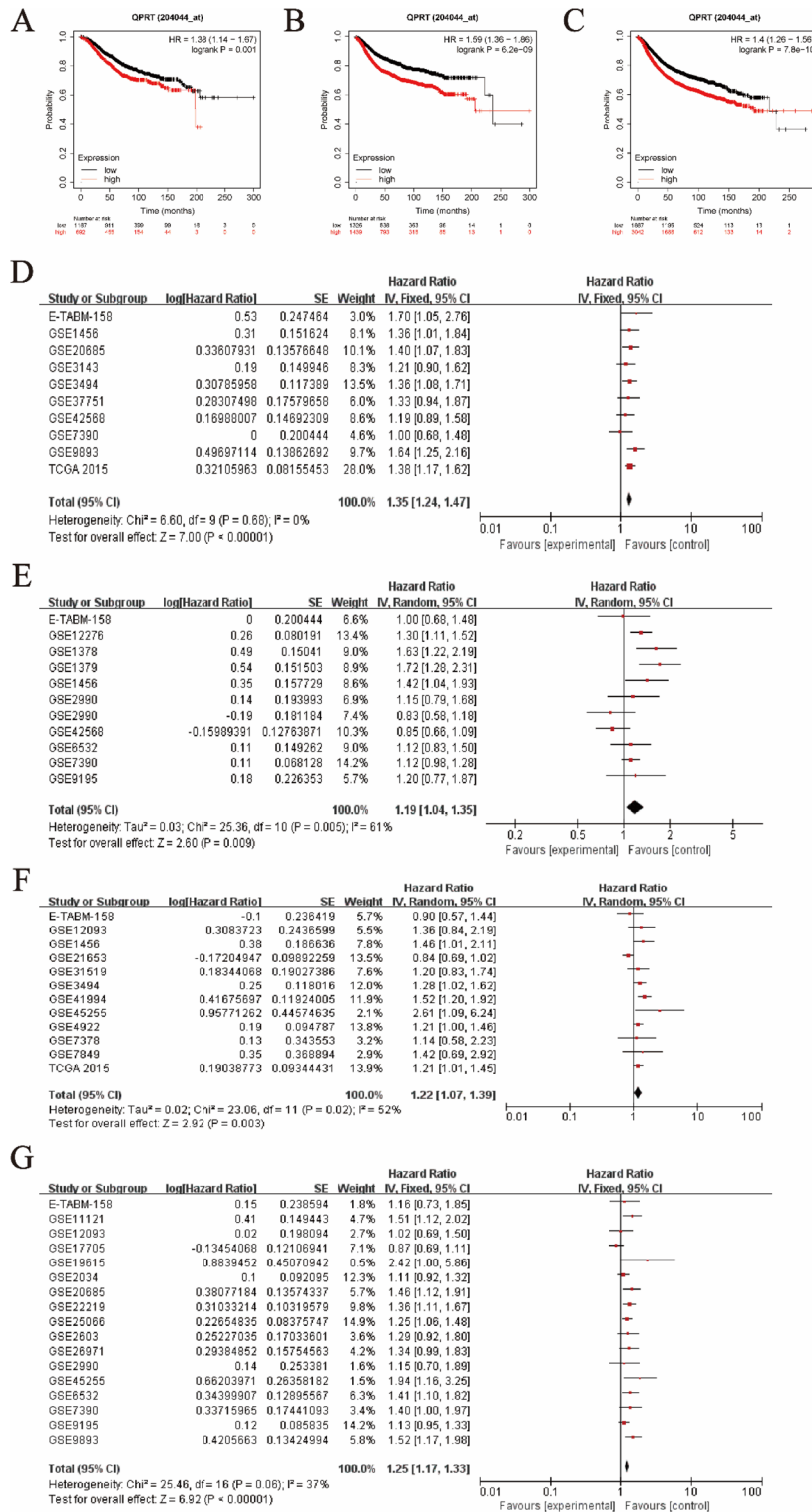


Figure 2. The relationship between QPRT expression and prognosis values in breast cancer. Overall survival (OS) between the high-low expression groups of QPRT gene in Kaplan–Meier Plotter. (B) Distant metastasis-free survival (DMFS) between the high-low expression groups of QPRT gene in Kaplan–Meier Plotter. (C) Relapse-free survival (RFS) between the high-low expression groups of QPRT gene in Kaplan–Meier Plotter. (D) Ten datasets (2822 samples) assessed the relationship between QPRT and overall survival. (E) Eleven datasets (2085 samples) assessed the relationship between QPRT and recurrence-free survival. (F) Twelve datasets (3180 samples) assessed the relationship between QPRT and disease-free survival. (G) Seventeen datasets (4100 samples) assessed the relationship between QPRT and distant metastasis-free survival.

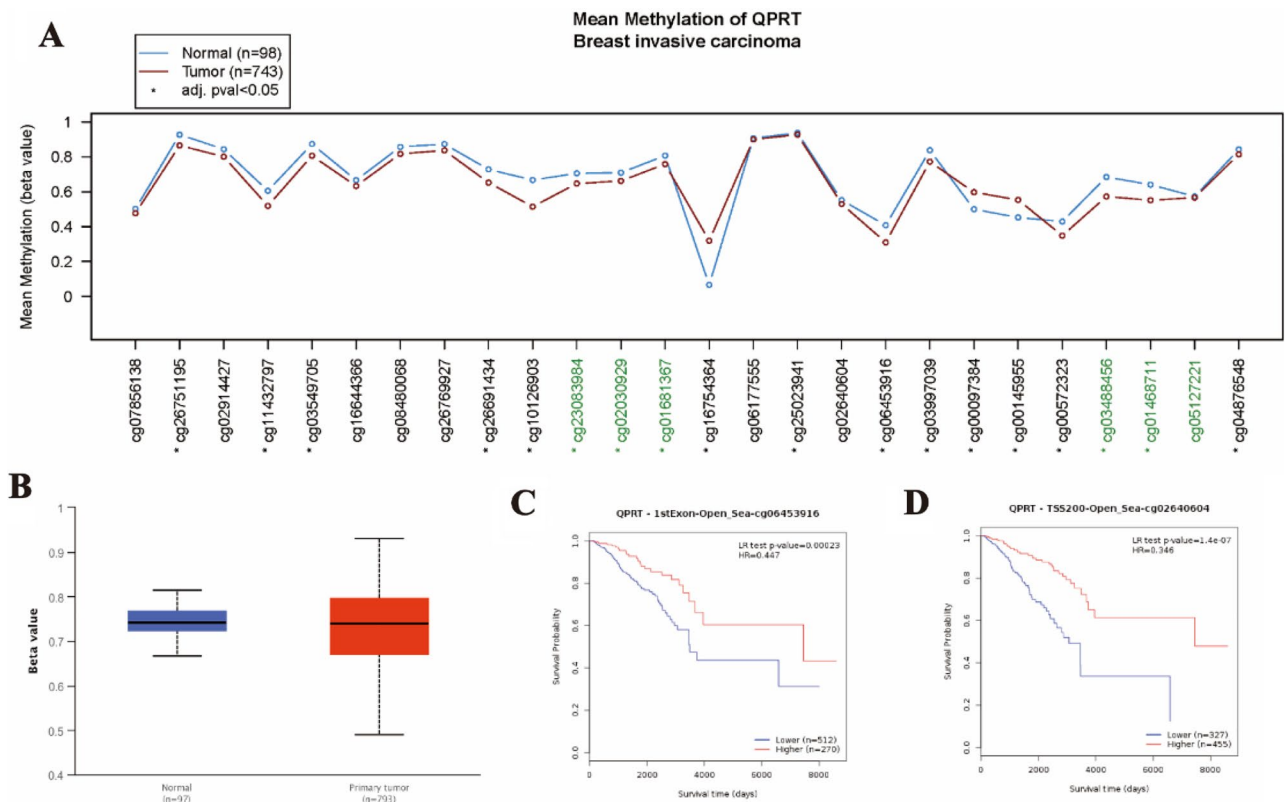


Figure 3. The methylation level of QPRT and prognosis in breast cancer. **(A)** The mean methylation of QPRT in breast cancer showed from the MethSurv database. **(B)** The promotor expression levels of QPRT between primary tumor and normal breast cancer tissues in TCGA were analyzed by the UALCAN database. **(C)** The relationship between QPRT methylation level and OS (cg06453916). **(D)** The relationship between QPRT methylation level and OS (cg02640602).

By analysing the GEO dataset GSE151521, we identified several QPRT knockdown related genes and conducted enrichment analysis. We found that the knockdown of QPRT significantly enriched terms related to the Wnt signalling pathway, MAPK signalling pathway, cell cycle, and cell proliferation in GO enrichment analysis. Additionally, macrophage-related enrichment in the immune response occurred frequently (Fig. 5A). In KEGG enrichment analysis, we observed enrichment in pathways such as the Wnt signalling pathway, PPAR signalling pathway, PI3K-AKT signalling pathway, and apoptosis (Fig. 5B). Both QPRT-related genes in the LinkedOmics database and genes associated with QPRT knockdown showed correlations with the Wnt signalling pathway and cell cycle. We speculate that QPRT may play a role in breast cancer through the regulation of the cell cycle and modulation of molecules in the Wnt signalling pathway.

The relationship between QPRT single-cell analyses and immune infiltrate abundances in breast cancer. Based on the human protein atlas data, breast tissue could be divided into 25 clusters by single-cell sequencing analysis. In these 25 clusters, QPRT was mainly highly expressed in fibroblasts, B cells, and macrophages (Fig. 6A). Furthermore, single-cell sequencing of other tissues found that QPRT was highly expressed in macrophages (Fig. S5). This suggested that QPRT may affect the microenvironment, through macrophages, to promote or inhibit the occurrence of disease.

To visualize the correlation between QPRT expression and immune infiltration levels in breast cancer, a large number of available TCGA samples were used. QPRT was positively associated with monocyte cell ($r = 0.12$, $P = 1.3e-04$), M2 macrophage cell ($r = 0.23$, $P = 4.9e-02$) (Fig. 6B), central memory CD4+ T-cell ($r = 0.38$, $P = 2.1e-03$), B-cell ($r = 0.19$, $P = 7.5e-06$), NK cell ($r = 0.16$, $P = 2.3e-02$), neutrophil cell ($r = 0.15$, $P = 4.6e-02$), myeloid dendritic cell ($r = 0.15$, $P = 7.0e-04$), T-cell of NK ($r = 0.15$, $P = 8.4e-04$), follicular helper T-cell ($r = 0.12$, $P = 5.5e-03$), MDSC (myeloid-derived suppressor cells) ($r = 0.12$, $P = 7.6e-03$) and regulatory T-cell ($r = 0.11$, $P = 1.5e-02$) infiltration but negatively associated with mast cell ($r = -0.17$, $P = 1.9e-02$), CD8+ T-cell ($r = -0.36$, $P = 1.9e-03$), haematopoietic stem cell ($r = -0.11$, $P = 4.6e-04$), common lymphoid progenitor ($r = -0.18$, $P = 1.4e-02$) and granulocyte-monocyte progenitor ($r = -0.16$, $P = 3.3e-02$) (Fig. S6).

Moreover, the expression of QPRT in HER2+ breast cancer is significantly higher than that in other subtypes (Fig. 1B), so we chose to explore the relationship between QPRT and macrophages in HER2+ breast cancer. We found that higher expression of QPRT was found in M2 macrophages than in M0 macrophages by qPCR, and the same results were validated in the GSE159112 database (Fig. 6C). Furthermore, high QPRT expression was also found in TAMs (M0 macrophages cocultured with SK-BR-3 cell or BT-474 cell supernatants) compared

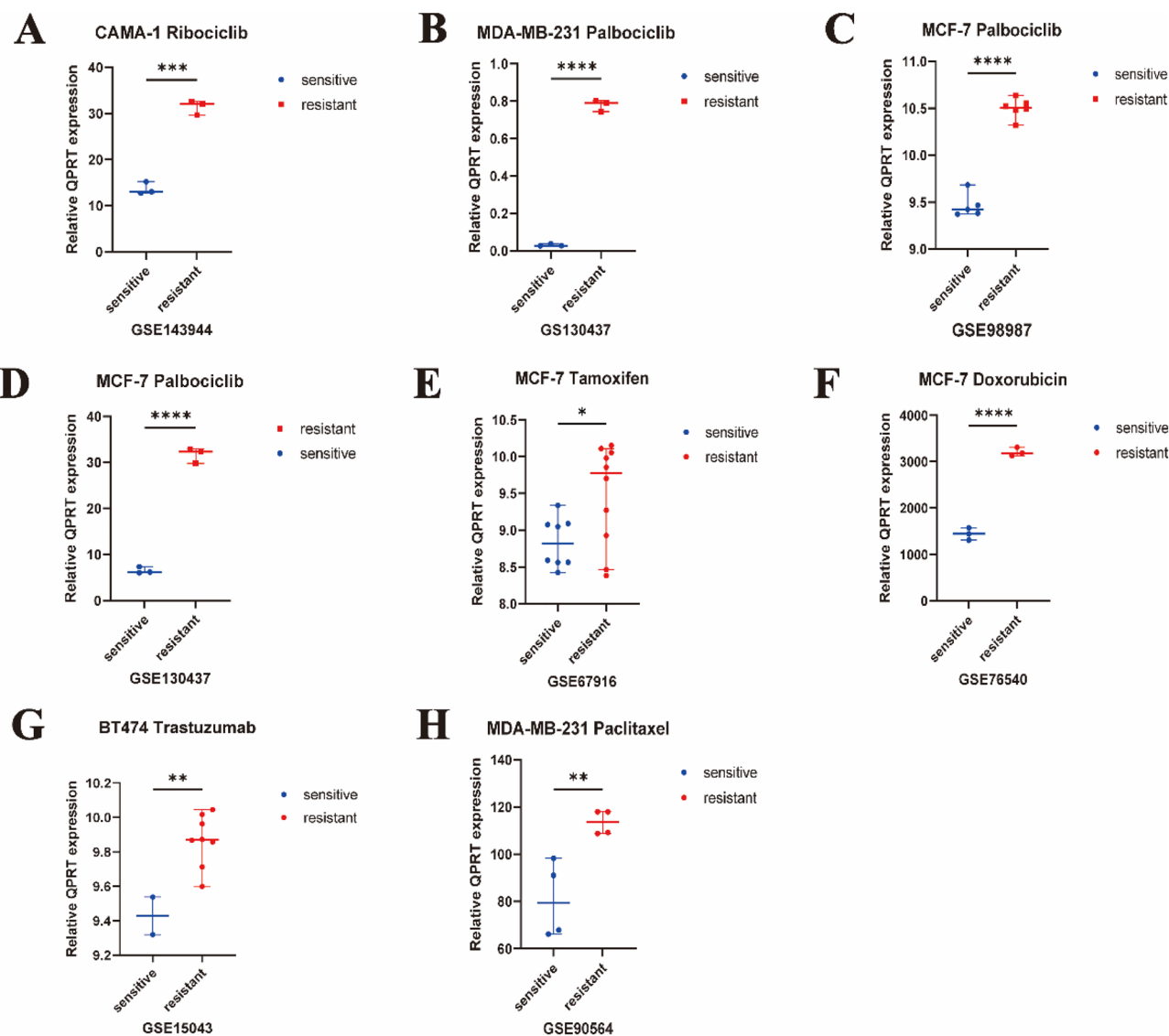


Figure 4. The expression of QPRT between acquired drug-resistant and sensitive cell lines. (A) The expression of QPRT between Ribociclib-resistant and sensitive CAMA-1 cell line in GSE143944. (B) The expression of QPRT between Palbociclib-resistant and sensitive MDA-MB-231 cell line in GSE130437. (C) The expression of QPRT between Palbociclib-resistant and sensitive MCF-7 cell line in GSE98987. (D) The expression of QPRT between Palbociclib-resistant and sensitive MCF-7 cell line in GSE130437. (E) The expression of QPRT between Tamoxifen-resistant and sensitive MCF-7 cell line in GSE67916. (F) The expression of QPRT between Doxorubicin-resistant and sensitive MCF-7 cell line in GSE76540. (G) The expression of QPRT between Trastuzumab-resistant and sensitive BT474 cell line in GSE15043. (H) The expression of QPRT between Paclitaxel-resistant and sensitive MDA-MB-231 cell line in GSE90564. Two-tailed unpaired Student's *t*-test was used to calculate *P* values. (A)–(D) Data are presented as the median \pm 95% CI. **P* < 0.05 ***P* < 0.01 *** *P* value < 0.001, **** *P* < 0.0001.

with M0 macrophages in HER2+ breast cancer. Similar expression changes were also observed in the GSE115040 datasets (Fig. 6D).

The correlation of QPRT expression with biomolecules and comparative toxicogenomics. To predict miRNA binding sites related to QPRT, we explored the TargetScan database and found that 612 miRNAs might regulate QPRT. The most likely targets in these sites were hsa-miR-4763-5p, hsa-miR-7973, hsa-miR-4674, hsa-miR-4437, hsa-miR-4468, hsa-miR-4701-5p and hsa-miR-3189-5p (context ++ score < -0.5 and context ++ score percentile > 99) (Fig. 7A). To further explore possible drug targets of QPRT, the Comparative Toxicogenomics Database (CTD) was used. The results visualized by Cytoscape showed that a series of drugs can target QPRT, such as antineoplastic drugs such as cisplatin, Jinfukang, flutamide, and entinostat and substances in the human body such as oestradiol, lactic acid, and testosterone (Fig. 7B). The intersection of the above results and the results of the CMAP website analysis found that these drugs appeared repeatedly, including



Figure 5. The function prediction results of QPRT in breast cancer. (A) Significantly enriched GO terms and (B) top enriched KEGG pathways were showed by analyzing GEO dataset (GSE 151521).

clofibrate, cytarabine, entinostat, estradiol, flutamide, niacin, resveratrol, rosiglitazone, testosterone, tretinoin and valdecoxib. This suggests that QPRT is more likely to be associated with these drugs and affect breast cancer directly or indirectly. In addition, based on the three databases of iRefIndex, BioGrid and IMEx, we draw the protein-protein interaction networks (PPI) related to QPRT respectively (Fig. 7C–E). We summarized the results of these three databases and found that these genes or proteins appeared in these three databases, including PKLR, AMBP, APOC3, RBP4, APOM, TF, UBE2J1, DNAJB9, SEC61B, HILPDA, LIPA, YIPF5, SEC23IP and

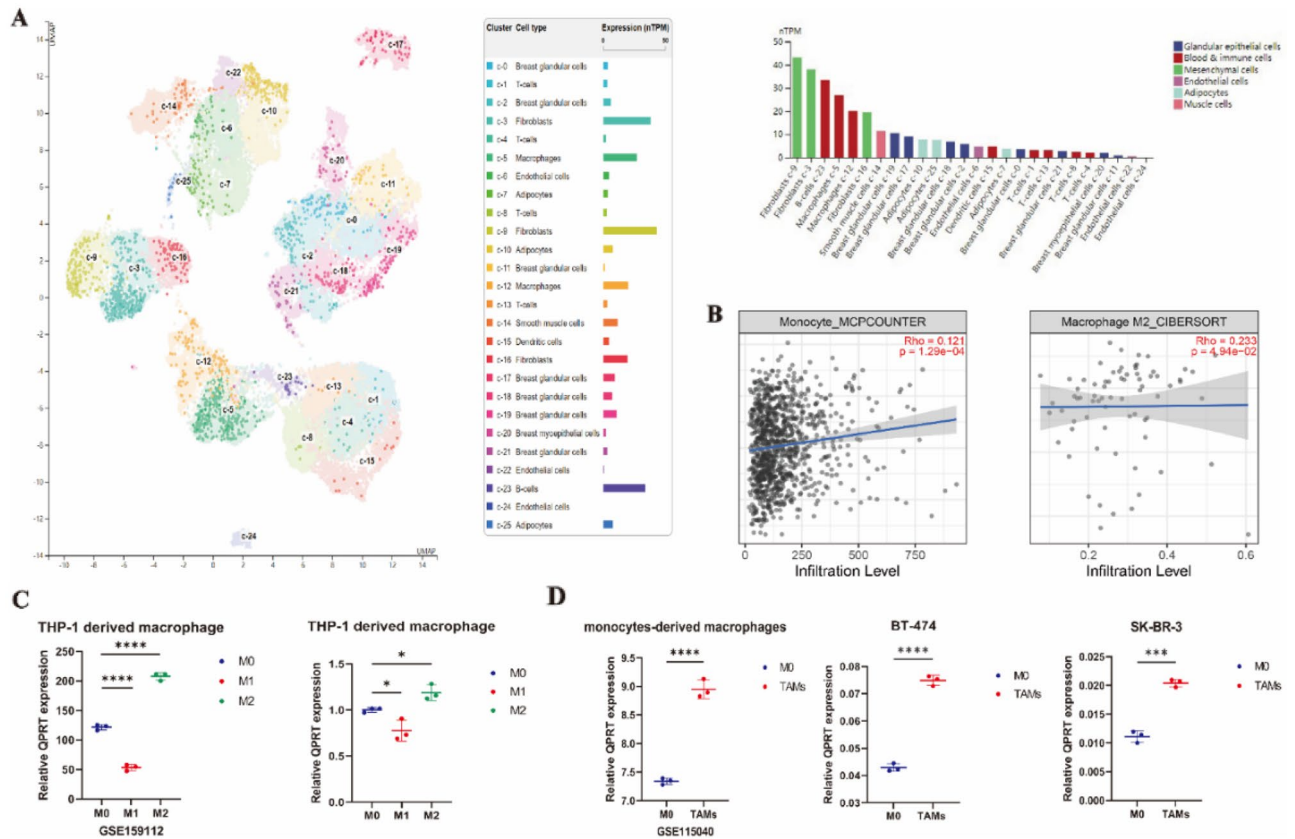


Figure 6. The relationship between QPRT single-cell analyses and immune infiltrates' abundances in breast cancer. **(A)** The relationship between QPRT expression and different single-cell types in breast tissues. **(B)** The relationship between QPRT and different macrophage cell infiltration. **(C)** M0 macrophages: PMA-stimulated THP-1 cells for 48 h (PMA 100 ng/ml), M1 macrophages: LPS (100 ng/ml) and IFN- γ (20 ng/ml) induce M0 macrophages to M1-like phenotype, M2 macrophages: IL-4(20 ng/ml) and IL-13(20 ng/ml) induce M0 macrophages to M2-like phenotype, TAMs (tumor-associated macrophages): culture supernatant of SK-BR-3 cells or BT-474 cells were added in M0 macrophages in proportion co-culture for 48 h. The scatter plot shows the expression of QPRT among M0 macrophages, M2 macrophages, and TAMs. Two-tailed unpaired Student's t-test was used to calculate *P* values. **(D)** The expression of QPRT among M0 macrophages, M2 macrophages, and TAMs in GEO. **(C,D)** Data are presented as the mean \pm 95% CI. ***P* < 0.01, ****P* < 0.001, *****P* < 0.0001.

SEC24C. We reasonably believe that QPRT is likely to interact with these genes or proteins and affect the progression of breast cancer. We speculated that these biomolecules and comparative toxicogenomics can prevent breast cancer deterioration and even improve patient survival status.

Discussion

QPRT is the key enzyme in the catabolism of quinolinic acid, which is known as an intermediate in the kynurenine pathway of tryptophan to nicotinamide adenine dinucleotide (NAD). Regarding this tryptophan metabolic pathway, many studies have already shown that tryptophan metabolism plays an important role in cancer progression by inhibiting the antitumour immune response and promoting the malignant characteristics of cancer cells. It was reported that degrading enzymes in the kynurenine pathway were expressed in various types of cancer and related to adverse clinical outcomes²⁹. There is evidence showing that NAD⁺ exerts a role in tumour biology through tryptophan and that inhibition of de novo NAD⁺ synthesis promotes tumourigenesis through DNA damage in the liver³⁰. Additionally, some research has shown that the metabolite of tryptophan can promote the movement and metastasis of cancer cells in glioblastoma³¹ and breast cancer³². Moreover, accumulation of endogenous tryptophan-derived metabolites³³, immune-related effects³⁴, and expression status³⁵ had influences on breast cancer, although kynurenic acid had not been previously associated with breast cancer risk³⁶. The potential mechanisms of this metabolic pathway mediating disease include tryptophan-dependent protein toxicity, excitatory toxicity caused by the accumulation of tryptophan metabolites, and energy imbalance caused by NAD⁺ depletion, containing local restrictive changes in downstream metabolites in the tumour microenvironment³⁷. Based on the above results, we believe that QPRT is potentially very important in the genesis, progression, metastasis, and invasion of breast cancer.

Liu et al. found that QPRT expression levels were upregulated in breast cancer and that knockdown of QPRT could inhibit breast cancer cell migration and invasion¹⁷. Upregulated QPRT promoted growth, migration, and

invasion and increased drug resistance¹⁰. Similarly, we found that the expression level of QPRT in breast cancer tissues was significantly higher than that in normal tissues. The UALCAN and bc-GenExMiner online tools revealed that HER2 positivity, nodal metastasis status, and TP53 mutation were positively correlated with high QPRT expression. We further investigated the prognostic value of QPRT in breast cancer using the Kaplan–Meier Plotter and bc-GenExMiner databases. Patients with high QPRT expression levels had worse survival prognosis in OS as well as DMFS and RFS, either ER+, PR+, and HER2+ receptor status or molecular subtyping. In ER+ breast cancer, DSCAM-AS1 increased QPRT expression and caused poor prognosis¹¹. These findings collectively demonstrated that QPRT might be a prognostic biomarker for breast cancer.

A previous study showed that overexpression of QPRT increased partial resistance to imatinib in K562 cells, suggesting that QPRT may have an anti-apoptotic function¹⁰. By using the ROC plotter online analysis tool, we demonstrated that taxane and anthracycline, as predictive biomarkers in breast cancer, were statistically significant with the area under the curve (AUC). Furthermore, we analysed GEO datasets and found that QPRT was able to be a biomarker for taxane, trastuzumab, paclitaxel, doxorubicin, and tamoxifen via acquired drug resistance. Coincidentally, we found that there was an obvious high relevance between QPRT and antineoplastic drugs such as cisplatin, Jinfukang, and entinostat by using the comparative toxicogenomics database (CTD) analysis tool. These findings indicate that QPRT may act as a potential target and biomarker to indicate drug resistance and the clinical efficacy of breast cancer antitumour drugs.

In our enrichment analysis of QPRT, a significant association with the cell cycle was observed. QPRT is capable of regulating the transition from G0 to G1 and influencing the G1/S transition of the mitotic cell cycle. By analyzing the GEO dataset, it was found that the expression of QPRT in the CDK4 / 6 inhibitor palbociclib resistance group was higher than that in the control group. Interestingly, we also identified a certain relationship between QPRT and the cell cycle drug cytarabine. It is well known that cytarabine, as a pyrimidine antimetabolite mainly targeting the S phase of cell proliferation in clinical settings, exerts a noticeable anti-tumour effect by inhibiting cell DNA synthesis and impeding cell proliferation³⁸. We hypothesize that QPRT is likely to be directly or indirectly involved in cell cycle regulation and consequently impacts the occurrence and progression of breast cancer.

It has been shown that QPRT promotes breast cancer progression by activating the PI3K/Akt pathway³⁹. Consistently, our study revealed a significant enrichment of QPRT in the PI3K-AKT signalling pathway. Moreover, QPRT is also associated with the gene-drug effects of resveratrol and estradiol. Resveratrol has been reported to induce apoptosis in cancer cells by downregulating PI3K, leading to cell cycle arrest⁴⁰. On the other hand, chronic exposure to high levels of estradiol has been identified as a major cause of ER-positive breast cancer⁴¹, and it can upregulate Twist via the PI3K/AKT/NF- κ B signalling pathway, thereby promoting the progression of hormone-dependent breast cancer⁴². These findings further support the notion that QPRT can influence the progression of breast cancer through the PI3K-AKT signalling pathway.

Additionally, rosiglitazone, a drug used for diabetes treatment, has shown positive anti-tumour effects in breast cancer. Research has demonstrated that the combination of rosiglitazone with MEK inhibitors can induce the differentiation of breast cancer cells into adipocytes, reducing tumour invasiveness and suppressing tumour metastasis⁴³. In our study, we found that QPRT is significantly enriched in the PPAR signalling pathway and exhibits a relationship with rosiglitazone. It is possible that rosiglitazone and QPRT may also have a similar promoting or inhibitory relationship, thereby influencing the occurrence and development of tumours.

Jones et al. found that QPRT expression correlated significantly with neopterin, a pro-inflammatory immune response marker⁴⁴. In follicular thyroid carcinoma, QPRT might be a potential marker in immunohistochemical features⁴⁵. According to our results, QPRT was positively associated with the infiltration of many immune cells, such as central memory CD4+ T cells, regulatory T cells, M2 macrophages, B cells, monocytes, NK cells, and neutrophils, but negatively associated with mast cells and CD8+ T cells. Significantly, our enrichment analysis revealed the presence of various macrophage-related biological processes, including the Fc-gamma receptor signaling pathway associated with phagocytosis. Further investigation indicated that QPRT was more highly expressed in M2 macrophage cells than in M0 macrophage cells, and the expression of QPRT in two different tumour-associated macrophages was also higher than that in M0 macrophages. In terms of tumour growth, M2 macrophages can accelerate cancer cells growth by releasing growth factors⁴⁶. Promoting M2 polarization or increasing the ratio of M2/M1 can promote tumour proliferation and development^{47–52}, and M2-polarized macrophages have obvious proangiogenic and protumorigenic effects⁵³. In terms of tumour invasion and metastasis, increased M2 macrophages in the tumour immune microenvironment can drive breast cancer metastasis⁵⁴. Tumour-promoting M2 macrophages enriched in the tumour microenvironment increase the invasiveness of triple-negative breast cancer (TNBC)⁵⁵, and CHI3L1 secreted by M2 macrophages promotes the metastasis of gastric cancer and breast cancer cells in vitro and in vivo⁵⁶. In addition, studies have shown that M2 macrophages are associated with poor prognoses in tumours, such as TNBC⁵⁷ and oral squamous cell carcinoma⁵⁰. Immunosuppression is also a known effect of M2 macrophages, which can damage the antitumour immunity of the tumour microenvironment^{58–60}. In tumour treatment resistance and drug resistance, M2 macrophages can not only promote the chemotherapy resistance of cancer cells⁶¹ but also mediate the radiation resistance of inflammatory breast cancer (IBC) cells with cocultured IBC cell lines⁶². Studies have shown that QPRT overexpression activates the phagocytosis of macrophages and vice versa. Inhibition of QPRT increased the surface markers of M1 macrophages and decreased the surface markers of M2 macrophages⁶³. We reasonably suppose that QPRT may play a tumour-promoting role through M2 macrophages. Although in GSE55015⁶⁴, QPRT had meaningless miRNA and mRNA expression in vitro tumour-educated macrophages (TEM), the identified miRNAs through in vitro profiling of TEM had longer DFS in ER+ breast cancers. The results showed that under the effect of QPRT, breast cancer could be regulated by immune cells in development and prognosis.

QPRT has been reported, but only in a few types of cancers. Multiple genes or proteins interact with QPRT in different ways and participate in the occurrence, development, invasion, and metastasis of breast cancer, but few

have been verified. It is essential to predict the function and related molecules of QPRT. Identifying the function of QPRT will not only elucidate the role of the gene but will also provide ideas for potential therapeutic targets for research on new drugs and antitumour drug resistance.

Conclusion

QPRT may be a new target for breast cancer for both cancer cells and tumour-educated macrophages. QPRT was higher in breast cancer tissue, and its higher level represented worse survival. The worse survival of high QPRT might be due to acquired drug resistance to, for example, chemotherapy, trastuzumab, endocrine drugs, and CDK4/6 inhibitors. Meanwhile, QPRT might also activate the PI3K-AKT and cell cycle to accelerate tumour growth and survival. QPRT might be a biomarker for TAMs and M2 macrophages, and QPRT might function via the Fc-epsilon receptor signalling pathway in macrophages.

Data availability

The data used to support the findings of this study are included in the article.

Received: 12 May 2023; Accepted: 12 September 2023

Published online: 18 September 2023

References

- Sung, H. *et al.* Global Cancer Statistics 2020: GLOBOCAN Estimates of Incidence and Mortality Worldwide for 36 Cancers in 185 Countries. *CA: Cancer J. Clin.* **71**(3), 209–249 (2021).
- Yersal, O. & Barutca, S. Biological subtypes of breast cancer: Prognostic and therapeutic implications. *World J. Clin. Oncol.* **5**(3), 412–424 (2014).
- Emens, L. A. Breast cancer immunotherapy: Facts and hopes. *Clin. Cancer Res.: Off. J. Am. Assoc. Cancer Res.* **24**(3), 511–520 (2018).
- Prat, A. *et al.* Clinical implications of the intrinsic molecular subtypes of breast cancer. *Breast (Edinburgh, Scotland)*. **24**(Suppl 2), S26–35 (2015).
- Bredin, P., Walshe, J. M. & Denduluri, N. Systemic therapy for metastatic HER2-positive breast cancer. *Semin. Oncol.* **47**(5), 259–269 (2020).
- Dillekäs, H., Rogers, M. S. & Straume, O. Are 90% of deaths from cancer caused by metastases?. *Cancer Med.* **8**(12), 5574–5576 (2019).
- Shaffer, S. M. *et al.* Rare cell variability and drug-induced reprogramming as a mode of cancer drug resistance. *Nature* **546**(7658), 431–435 (2017).
- Chun, K. H., Park, J. H. & Fan, S. Predicting and overcoming chemotherapeutic resistance in breast cancer. *Adv. Exp. Med. Biol.* **1026**, 59–104 (2017).
- Sledge, G. W. *et al.* Past, present, and future challenges in breast cancer treatment. *J. Clin. Oncol.: Off. J. Am. Soc. Clin. Oncol.* **32**(19), 1979–1986 (2014).
- Ullmark, T. *et al.* Anti-apoptotic quinolinate phosphoribosyltransferase (QPRT) is a target gene of Wilms' tumor gene 1 (WT1) protein in leukemic cells. *Biochem. Biophys. Res. Commun.* **482**(4), 802–807 (2017).
- Yue, Z. *et al.* Silencing DSCAM-AS1 suppresses the growth and invasion of ER-positive breast cancer cells by downregulating both DCTPP1 and QPRT. *Aging* **12**(14), 14754–14774 (2020).
- Chandrashekar, D. S. *et al.* UALCAN: A portal for facilitating tumor subgroup gene expression and survival analyses. *Neoplasia (New York, NY)*. **19**(8), 649–658 (2017).
- Jézéquel, P. *et al.* bc-GenExMiner: An easy-to-use online platform for gene prognostic analyses in breast cancer. *Breast Cancer Res. Treat.* **131**(3), 765–775 (2012).
- Bartha, Á. & Györfy, B. TNMplot.com: A Web tool for the comparison of gene expression in normal, tumor and metastatic tissues. *Int. J. Mol. Sci.* **22**(5), 2622 (2021).
- Györfy, B. Survival analysis across the entire transcriptome identifies biomarkers with the highest prognostic power in breast cancer. *Comput. Struct. Biotechnol. J.* **19**, 4101–4109 (2021).
- Vasaikar, S. V., Straub, P., Wang, J. & Zhang, B. LinkedOmics: analyzing multi-omics data within and across 32 cancer types. *Nucleic Acids Res.* **46**(D1), D956–D963 (2018).
- Liu, C. L. *et al.* Quinolinate phosphoribosyltransferase promotes invasiveness of breast cancer through myosin light chain phosphorylation. *Front. Endocrinol.* **11**, 621944 (2020).
- da Huang, W., Sherman, B. T. & Lempicki, R. A. Bioinformatics enrichment tools: Paths toward the comprehensive functional analysis of large gene lists. *Nucleic Acids Res.* **37**(1), 1–13 (2009).
- Bu, D. *et al.* KOBAS-i: intelligent prioritization and exploratory visualization of biological functions for gene enrichment analysis. *Nucleic Acids Res.* **49**(W1), W317–W325 (2021).
- Kanehisa, M., Furumichi, M., Sato, Y., Kawashima, M. & Ishiguro-Watanabe, M. KEGG for taxonomy-based analysis of pathways and genomes. *Nucleic Acids Res.* **51**(D1), D587–D592 (2023).
- Modhukur, V. *et al.* MethSurv: a web tool to perform multivariable survival analysis using DNA methylation data. *Epigenomics* **10**(3), 277–288 (2018).
- Diez-Villanueva, A., Mallona, I. & Peinado, M. A. Wanderer, an interactive viewer to explore DNA methylation and gene expression data in human cancer. *Epigenet. Chromatin* **8**, 22 (2015).
- Fekete, J. T. & Györfy, B. ROCplot.org: Validating predictive biomarkers of chemotherapy/hormonal therapy/anti-HER2 therapy using transcriptomic data of 3104 breast cancer patients. *Int. J. Cancer.* **145**(11), 3140–3151 (2019).
- Karlsson, M. *et al.* A single-cell type transcriptomics map of human tissues. *Sci. Adv.* **7**(31), eabh2169 (2021).
- Li, T. *et al.* TIMER2.0 for analysis of tumor-infiltrating immune cells. *Nucleic Acids Res.* **48**(W1), W509–W514 (2020).
- Agarwal, V., Bell, G. W., Nam, J. W. & Bartel, D. P. Predicting effective microRNA target sites in mammalian mRNAs. *Elife* **4**, e05005 (2015).
- Gronin, C. J. *et al.* Predicting molecular mechanisms, pathways, and health outcomes induced by Juul e-cigarette aerosol chemicals using the Comparative Toxicogenomics Database. *Curr. Res. Toxicol.* **2**, 272–281 (2021).
- Lamb, J. *et al.* The Connectivity Map: Using gene-expression signatures to connect small molecules, genes, and disease. *Science (New York, NY)*. **313**(5795), 1929–1935 (2006).
- Opitz, C. A. *et al.* The indoleamine-2,3-dioxygenase (IDO) inhibitor 1-methyl-D-tryptophan upregulates IDO1 in human cancer cells. *PLoS ONE* **6**(5), e19823 (2011).
- Tummala, K. S. *et al.* Inhibition of de novo NAD(+) synthesis by oncogenic URI causes liver tumorigenesis through DNA damage. *Cancer Cell* **26**(6), 826–839 (2014).

31. Ott, M. *et al.* Suppression of TDO-mediated tryptophan catabolism in glioblastoma cells by a steroid-responsive FKBP52-dependent pathway. *Glia* **63**(1), 78–90 (2015).
32. D'Amato, N. C. *et al.* A TDO2-AhR signaling axis facilitates anoikis resistance and metastasis in triple-negative breast cancer. *Can. Res.* **75**(21), 4651–4664 (2015).
33. Puccetti, P. *et al.* Accumulation of an endogenous tryptophan-derived metabolite in colorectal and breast cancers. *PLoS ONE* **10**(4), e0122046 (2015).
34. Levina, V., Su, Y. & Gorelik, E. Immunological and nonimmunological effects of indoleamine 2,3-dioxygenase on breast tumor growth and spontaneous metastasis formation. *Clin. Dev. Immunol.* **2012**, 173029 (2012).
35. Dewi, D. L. *et al.* Suppression of indoleamine-2,3-dioxygenase 1 expression by promoter hypermethylation in ER-positive breast cancer. *Oncoimmunology*. **6**(2), e1274477 (2017).
36. Zeleznik, O. A. *et al.* Circulating amino acids and amino acid-related metabolites and risk of breast cancer among predominantly premenopausal women. *NPJ Breast Cancer*. **7**(1), 54 (2021).
37. Platten, M., Nollen, E. A. A., Röhrig, U. F., Fallarino, F. & Opitz, C. A. Tryptophan metabolism as a common therapeutic target in cancer, neurodegeneration and beyond. *Nat. Rev. Drug Discovery* **18**(5), 379–401 (2019).
38. Bosnjak, M. *et al.* Inhibition of mTOR-dependent autophagy sensitizes leukemic cells to cytarabine-induced apoptotic death. *PLoS ONE* **9**(4), e94374 (2014).
39. Zhou, L., Mu, L., Jiang, W. & Yang, Q. QPRT acts as an independent prognostic factor in invasive breast cancer. *J. Oncol.* **2022**, 6548644 (2022).
40. Han, Y., Jo, H., Cho, J. H., Dhanasekaran, D. N. & Song, Y. S. Resveratrol as a tumor-suppressive nutraceutical modulating tumor microenvironment and malignant behaviors of cancer. *Int. J. Mol. Sci.* **20**(4), 925 (2019).
41. Peng, B. L. *et al.* A hypermethylation strategy utilized by enhancer-bound CARM1 to promote estrogen receptor α -dependent transcriptional activation and breast carcinogenesis. *Theranostics*. **10**(8), 3451–3473 (2020).
42. Han, R. *et al.* Estrogen promotes progression of hormone-dependent breast cancer through CCL2-CCR2 axis by upregulation of Twist via PI3K/AKT/NF- κ B signaling. *Sci. Rep.* **8**(1), 9575 (2018).
43. Ishay-Ronen, D. *et al.* Gain fat-lose metastasis: Converting invasive breast cancer cells into adipocytes inhibits cancer metastasis. *Cancer Cell* **35**(1), 17–32.e6 (2019).
44. Jones, S. P. *et al.* Expression of the Kynurenine pathway in human peripheral blood mononuclear cells: implications for inflammatory and neurodegenerative disease. *PLoS ONE* **10**(6), e0131389 (2015).
45. Hirsch, N., Frank, M., Döring, C., Vorländer, C. & Hansmann, M. L. QPRT: a potential marker for follicular thyroid carcinoma including minimal invasive variant; a gene expression, RNA and immunohistochemical study. *BMC Cancer* **9**, 93 (2009).
46. Siveen, K. S. & Kuttan, G. Role of macrophages in tumour progression. *Immunol. Lett.* **123**(2), 97–102 (2009).
47. Xiao, M. *et al.* SENP3 loss promotes M2 macrophage polarization and breast cancer progression. *Mol. Oncol.* **16**(4), 1026–1044 (2022).
48. Zhang, J. *et al.* Tumoral NOX4 recruits M2 tumor-associated macrophages via ROS/PI3K signaling-dependent various cytokine production to promote NSCLC growth. *Redox Biol.* **22**, 101116 (2019).
49. Yamaguchi, T. *et al.* Tumor-associated macrophages of the M2 phenotype contribute to progression in gastric cancer with peritoneal dissemination. *Gastric Cancer: Off. J. Int. Gastric Cancer Assoc. Jpn. Gastric Cancer Assoc.* **19**(4), 1052–1065 (2016).
50. Dan, H. *et al.* RACK1 promotes cancer progression by increasing the M2/M1 macrophage ratio via the NF- κ B pathway in oral squamous cell carcinoma. *Mol. Oncol.* **14**(4), 795–807 (2020).
51. Yao, Y., Xu, X. H. & Jin, L. Macrophage polarization in physiological and pathological pregnancy. *Front. Immunol.* **10**, 792 (2019).
52. Wang, L. X., Zhang, S. X., Wu, H. J., Rong, X. L. & Guo, J. M2b macrophage polarization and its roles in diseases. *J. Leukoc. Biol.* **106**(2), 345–358 (2019).
53. Zong, S., Dai, W., Guo, X. & Wang, K. LncRNA-SNHG1 promotes macrophage M2-like polarization and contributes to breast cancer growth and metastasis. *Aging* **13**(19), 23169–23181 (2021).
54. Zhang, M. *et al.* CECR2 drives breast cancer metastasis by promoting NF- κ B signaling and macrophage-mediated immune suppression. *Sci. Transl. Med.* **14**(630), eabf5473 (2022).
55. Weng, Y. S. *et al.* MCT-1/miR-34a/IL-6/IL-6R signaling axis promotes EMT progression, cancer stemness and M2 macrophage polarization in triple-negative breast cancer. *Mol. Cancer* **18**(1), 42 (2019).
56. Chen, Y., Zhang, S., Wang, Q. & Zhang, X. Tumor-recruited M2 macrophages promote gastric and breast cancer metastasis via M2 macrophage-secreted CHI3L1 protein. *J. Hematol. Oncol.* **10**(1), 36 (2017).
57. Bao, X. *et al.* Integrated analysis of single-cell RNA-seq and bulk RNA-seq unravels tumour heterogeneity plus M2-like tumour-associated macrophage infiltration and aggressiveness in TNBC. *Cancer Immunol. Immunother.: Clin.* **70**(1), 189–202 (2021).
58. Yu, T. *et al.* Modulation of M2 macrophage polarization by the crosstalk between Stat6 and Trim24. *Nat. Commun.* **10**(1), 4353 (2019).
59. Noy, R. & Pollard, J. W. Tumor-associated macrophages: from mechanisms to therapy. *Immunity* **41**(1), 49–61 (2014).
60. Colegio, O. R. *et al.* Functional polarization of tumour-associated macrophages by tumour-derived lactic acid. *Nature* **513**(7519), 559–563 (2014).
61. An, Y. & Yang, Q. MiR-21 modulates the polarization of macrophages and increases the effects of M2 macrophages on promoting the chemoresistance of ovarian cancer. *Life Sci.* **242**, 117162 (2020).
62. Rahal, O. M. *et al.* Blocking interleukin (IL)4- and IL13-mediated phosphorylation of STAT6 (Tyr641) decreases M2 polarization of macrophages and protects against macrophage-mediated radioresistance of inflammatory breast cancer. *Int. J. Radiat. Oncol. Biol. Phys.* **100**(4), 1034–1043 (2018).
63. Minhas, P. S. *et al.* Macrophage de novo NAD(+) synthesis specifies immune function in aging and inflammation. *Nat. Immunol.* **20**(1), 50–63 (2019).
64. Bleckmann, A. *et al.* Integrated miRNA and mRNA profiling of tumor-educated macrophages identifies prognostic subgroups in estrogen receptor-positive breast cancer. *Mol. Oncol.* **9**(1), 155–166 (2015).

Acknowledgements

The authors gratefully acknowledge the financial support by the Scientific Research Launch Project for new employees of the Second Xiangya Hospital of Central South University (2022-086), the Guangdong Provincial Laboratory of Advanced Energy Science and Technology (XJNY-2020434), the Natural Science Foundation of Hunan Province of China (2020JJ4828), the Science and Technology Innovation Program of Hunan Province (2021SK2026), the Health and Family Planning Commission of Hunan Province (2022JJ70143), the Tumor clinical research of Public welfare of Xiaoxiang (HTSF202207275503) and the Graduate Research and Innovation Projects of Hunan Province of China (2020zzts254).

Author contributions

W.J.Y. and L.L. designed the study. Y.Q.Y., Z.X.W., Y.C.Y., and Z.K.X. searched literature. Y.Q.Y., J.P., and X.Y.G. analyzed experimental results. Y.Q.Y. and L.L. wrote the manuscript.

Funding

This work was supported by the following funding projects, including the Scientific Research Launch Project for new employees of the Second Xiangya Hospital of Central South University (2022-086), the Guangdong Provincial Laboratory of Advanced Energy Science and Technology (XJNY-2020434), the Natural Science Foundation of Hunan Province of China (2020JJ4828), the Science and Technology Innovation Program of Hunan Province (2021SK2026), the Health and Family Planning Commission of Hunan Province (2022JJ70143), the Tumor clinical research of Public welfare of Xiaoxiang (HTSF202207275503) and the Graduate Research and Innovation Projects of Hunan Province of China (2020zzts254).

Competing interests

The authors declare no competing interests.

Additional information

Supplementary Information The online version contains supplementary material available at <https://doi.org/10.1038/s41598-023-42566-4>.

Correspondence and requests for materials should be addressed to Z.X. or W.Y.

Reprints and permissions information is available at www.nature.com/reprints.

Publisher's note Springer Nature remains neutral with regard to jurisdictional claims in published maps and institutional affiliations.



Open Access This article is licensed under a Creative Commons Attribution 4.0 International License, which permits use, sharing, adaptation, distribution and reproduction in any medium or format, as long as you give appropriate credit to the original author(s) and the source, provide a link to the Creative Commons licence, and indicate if changes were made. The images or other third party material in this article are included in the article's Creative Commons licence, unless indicated otherwise in a credit line to the material. If material is not included in the article's Creative Commons licence and your intended use is not permitted by statutory regulation or exceeds the permitted use, you will need to obtain permission directly from the copyright holder. To view a copy of this licence, visit <http://creativecommons.org/licenses/by/4.0/>.

© The Author(s) 2023